Electroencephalographic Phase–Amplitude Coupling in Simulated Driving With Varying Modality-Specific Attentional Demand

Ernesto Gonzalez-Trejo, Hannes Mögele, Norbert Pfleger, Ronny Hannemann, and Daniel J. Strauss

***Abstract*—The quantification of attention during driving can help identify situations in which the driver is not completely aware of the situation. By using the principle of phase–amplitude coupling (PAC) in electroencephalographic (EEG) signals, we aimed to test if PAC might be eligible as a biomarker of attention in multimodal tasks such as driving. Surface EEG was measured simultaneously in drivers and copilots while participating in simulated driving scenarios with varying multimodal attentional demands. The PAC between Theta-band phase and Gamma-band amplitude from the EEG was obtained and evaluated. Results showed significant PAC differences between drivers and copilots in areas related to multimodal attention (prefrontal cortex, frontal eye fields, primary motor cortex, and visual cortex). The results were confirmed by behavioral data acquired during the test (detection task). We conclude that PAC does function as a biomarker for attentional demand by detecting cortical areas being activated through specific multimodal (in this case, driving) tasks.**

***Index Terms*—Attention, driving, electroencephalography (EEG), phase–amplitude coupling (PAC).**

I. Introduction

DRIVING is a complex cognitive task, involving audiovisual cues, mechanical coordination, decision making, and information retention, among others, which have to be processed simultaneously [1]. Attention during driving is critical; even a slight distraction can lead to a dangerous situation. Current technological advances, such as navigation systems, hands-free systems, smart cockpits, and smartphone interfaces, aim to support driving tasks, but might actually act as a distraction [2]–[5]. Moreover, these interfaces might overlap additional distraction sources, such as passengers, fatigue effects, weather and/or traffic conditions, all inherent to driving [6]–[8].

The current challenge for physicians and researchers lies in the assessment of perceptual and cognitive workload and attention during a driving situation. Both functional magnetic resonance imaging (fMRI) [1], [9]–[12] and magnetoencephalography (MEG) [13]–[15] have been able to describe biomarkers such as Theta-band power increase and decrease correlated to active and passive driving [15], occipital brain activation during driving [1], [9], correlation of parietal–occipital and frontal lobe activation with steering operations [10], and decrease of parietal activity when distractions appear while driving (fMRI: [11], [12], MEG: [13], [14]); they have also shown a decrease in driving performance when engaged in tasks such as language comprehension [11] and conversation [13], which suggests a difference between external (driving task) and internal (cognitive task) attentional effort. However, these biomarkers have only been observed in a virtual environment due to the equipment required in order to acquire either fMRI or MEG. Portable solutions to study brain activity include electroencephalography (EEG) [16]–[22] and functional near infrared spectroscopy (fNIRS) [23]–[25]. These noninvasive methods allow for an easier setup and measurement of neural activity (e.g., using band power as a biomarker for attention) both in virtual and in real driving situations; although the information obtained is limited by the constraints of measuring neural activity at the scalp, both techniques provide a way to confirm results from imaging studies and allow for more flexible situations and novel study designs, which may even combine both EEG and fNIRS [26].

The analysis of EEG frequency band power has been commonly reported in the literature as a biomarker of neural activity related to attention while driving [22], [27]. For example, Gamma activity has been shown to correlate with sensory processing and both attentional and memory tasks [28]–[31], whereas Theta has been related with error processing, working memory, and information encoding [32]–[35], and Delta/Beta power spectra have been related to driving fatigue [22]. However, the reliability of band power alone has been questioned as it might reflect decreases in attention due to monotony, and not due to attentional resources being assigned to different cognitive tasks, as shown by [21]; their results suggest that the synchronization of oscillatory activity in the brain might offer a sounder alternative to quantify attention and cognitive effort.

Manuscript received June 13, 2018; revised December 28, 2018 and April 25, 2019; accepted June 30, 2019. This work was supported in part by the Federal Ministry of Education and Research (BMBF) Germany under Grant 03FH036I3 and in part by the German Research Foundation (DFG) under Grant STR 994/1-1. This article was recommended by Associate Editor Y. Li. *(Corresponding author: Daniel J. Strauss.)*

E. Gonzalez-Trejo and D. J. Strauss are with the Systems Neuroscience and Neurotechnology Unit, Saarland University and htw saar, 66421 Homburg/Saar, Germany (e-mail: ernesto.gonzaleztrejo@uni-saarland.de; daniel.strauss@uni-saarland.de).

H. Mögele is with the Audi Electronics Venture GmbH, 85080 Gaimersheim, Germany (e-mail: hannes.moegele@audi.de).

N. Pfleger is with the paragon semvox GmbH, 66459 Kirkel-Limbach, Germany (e-mail: pfleger@semvox.de).

R. Hannemann is with Sivantos GmbH, 91058 Erlangen, Germany (e-mail: ronny.hannemann@sivantos.com).

Color versions of one or more of the figures in this article are available online at http://ieeexplore.ieee.org.

Digital Object Identifier 10.1109/THMS.2019.2931011

Neuronal oscillations are the base of cognitive activity [36], [37], but the synchronization between different frequency bands is still being studied [38]. Cross-frequency coupling has received a lot of attention in recent years, by proving to be a biomarker of cognitive processing in humans [39]–[41]. Especially Theta–Gamma band coupling [42], [43], which has been related to sensory integration, working memory [44], [45], and visual perception [46], [47], which are essential for driving tasks [19]. Tort *et al.* proposed a new form of cross-frequency coupling, called phase–amplitude coupling (PAC) [42]. This coupling adapts the Kullback–Leiber (KL) distance measure [48] to calculate the deviation between the uniform distribution and an empirical amplitude distributionlike function projected over phase bins (in their original work, amplitude and phase information from *in vivo* hippocampal recordings) and assigns a modulation index to it (representing the amplitude–phase coupling intensity).

In this article, we obtained both the amplitude and phase information of surface EEG acquired during simulated driving (from both driver and copilot) and applied the framework established by Tort *et al.* to measure PAC. We aimed to test the feasibility of PAC as a biomarker of attention-related cortical activation in multimodal tasks (in our case, an audiovisual task while driving), both for active (driving) and passive (copilot) scenarios. We hypothesized that PAC would allow us to identify the cortical regions most active during attentional tasks. A behavioral task was also performed in order to confirm our main hypothesis. Moreover, we hypothesized that PAC could differentiate between auditory and visual attention based on the cortical activation observed. If confirmed, PAC, as obtained from surface EEG, could provide benefits such as portability, applicability in real-life situations, and noninvasiveness. Not only would PAC offer an alternative to analyze neural activity, but it might support all established biomarkers previously discussed as well.

II. Methods

A. Participants

Twenty two healthy subjects (three females), ages between 20 and 29 years (mean $= 24.4 \pm 2.7$ years), took part in the study. All subjects were right handed, German native speakers, and were required to have a valid driver's license (mean driving experience 6.8 ± 2.3 years); subjects were recruited from the social environment of the authors. The subjects had no hearing/visual impairments (contact lenses were allowed if they were required according to their driver's license). Before each measurement, the subjects were informed of the objectives and methodology of the measurement and asked to provide their written consent. No history of neurophysiological diseases/impairments was present in any of the subjects. The measurements were performed at the MINDSCAN Laboratory from the Systems Neuroscience and Neurotechnology Unit, Saarbruecken, Germany. The study was designed following ethic guidelines and the declaration of Helsinki; each participant was given the choice to abandon the measurement at any given time.

B. Driving Simulator

The indoor driving simulator consists of a real commercial vehicle cockpit (Audi A3, 2013) with an interface connected to a personal computer; the cockpit transfers information from the steering wheel and pedals to the simulation software (simulator interface and software from Simutech GmbH, Bremen, Germany). The software displays the virtual environment along three monitors. Driving in the simulation requires the same actions as real-life driving; the simulator is equipped with a manual, 5-gear gearbox transmission; all pedals (gas, brakes, and clutch) are functional. Speedometer and tachometer (RPM) are also connected to the software and display the speed/RPM in real time. The software simulation is able to render a small city, rural roads and/or highways, or a combination of them, according to the selected task. Pedestrians, traffic, and randomized events, such as pedestrian cross walks, wild animals, or construction sites, appear during driving and can be turned ON or OFF. Road navigation systems are also integrated (NAVI) and guide the subjects from the beginning to the end of the task through audiovisual cues (arrows displayed between speedometer and tachometer and auditory playback of spoken directions). Weather conditions (day/night, rain, snow, fog) can also be modified according to the task chosen.

The auditory output from the simulation software was rerouted to a separate personal computer, which was also used to playback additional auditory stimuli/tasks. A 24-loudspeaker array (JBL Control 1 Pro Loudspeakers, JBL, California, CA, USA) was mounted around the cockpit allowing for a directional control of auditory stimuli/distractions during driving. Each loudspeaker was controlled independently through audio-processing software (PreSonus Audio Electronics, Louisiana, LA, USA). Loudspeakers were arranged in three circular arrays, with a 45° angular resolution at floor (8 speakers, 40-cm high), ear (8 speakers, 115 cm) and over-the-head (8 speakers, 190 cm) heights. Both the audio coming from the driving simulator software as well as the audio used for auditory tasks were first converted to analog signals using a digital/analog interface (RME Digital/Analog Interface M-32 DA, RME Audio AG, Haimhausen, Germany). The loudspeakers were driven using three 8-channel audio amplifiers (Apart PA8250, Apart Audio NV, Antwerp, Belgium). Additionally, two subwoofer systems were embedded under the cockpit in order to elicit low-frequency vibration akin to the one present while driving. The subwoofers were driven using two additional audio amplifiers (the t.amp S-100 mk2, Thomann GmbH, Burgebrach, Germany; BKA 1000 N, The Guitammer Company, Ohio, OH, USA). Fig. 1 shows the layout of the driving simulator.

All audio tracks used were fine tuned and calibrated (intensity and position) to allow for a realistic spatial sound localization from the seat of the driver. This included varying amplitudes of combined speakers and cross mixing two or more speakers in order to enhance the directionality of the sound (e.g., sounds perceived as coming from the back seat or cockpit seat).

C. Driving Task

The driving task within all modalities of the study was to drive correctly (following traffic laws) around the selected environment, following the directions of the NAVI system. If a participant was seen deliberately disobeying traffic laws (e.g., speeding, driving on the wrong lane, running under red lights),

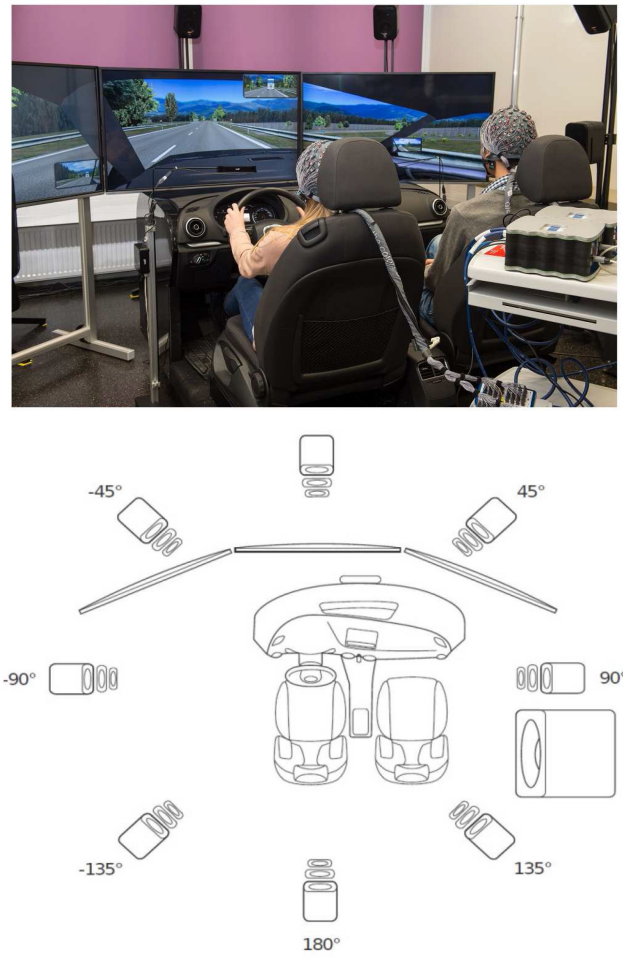

Fig. 1. Layout of driving simulator: (Top) A real automobile cockpit is used, together with software rendering a virtual environment on three monitors in front of the driver and a multidirectional speaker array, which provides auditory feedback, tasks, and distractions according to the task being presented. (Bottom) Speaker array: 24 speakers are arranged around the cockpit and allow for a flexible spatial localization of sounds. Several speakers can be linked together in order to simulate spatial localization more accurately (e.g., back seat or cockpit seat), or can be used independently. The subwoofer system under the cockpit is not shown.

the measurement was stopped and restarted after reminding the subject of the correct driving behavior expected. According to the selected task, the driving conditions changed (more/less traffic, bad weather) to increase or decrease the difficulty of the driving task. Additionally, eye-tracking hardware (Tobii Pro X2 60, Tobii AB, Sweden) was used to monitor the gaze of the subjects in real time and ensure that they were looking at the road during the measurement; both driver and copilot were reminded before each measurement to keep their eyes on the road during driving tasks.

D. Behavioral (Auditory) Task and Stimuli

The main auditory stimuli used for the behavioral tasks was a radio broadcast (in German) played while driving. According to the modality (scenario) of the study, the subjects were asked to detect a specific word within the broadcast ("und") and press a button, or do nothing and keep driving with the broadcast playback still ongoing. The word was chosen due to the number of occurrences in the selected radio broadcasts and due to being one of the most used words in German language [49]. This constituted the behavioral task of the study and was used to rate the difficulty of the driving situations; more difficult scenarios were expected to require more attention from the participants.

In order to increase the difficulty of the task, background noise was added. The main component of the background noise was the so-called "Fastl noise" [50], which simulates spectral and temporal features of human speech. This noise was implemented in the same loudspeakers as the radio broadcast. Additional auditory distracters were implemented, coming from different directions—recordings of babies crying and kids arguing were played from the loudspeakers simulating the back seats, while mobile-phone ringtones were played from the side loudspeakers to appear coming from the seat next to the driver. The sounds were evenly distributed along the task length, and special care was taken to ensure that none of the distracters overlapped the target words. All sounds were calibrated in order to attain safe hearing amplitude levels and were strictly kept under 80 dB sound pressure level (SPL). The maximum amplitude recorded (driving at maximum speed, with all auditory stimuli being played at the same time) was 72.3 dB SPL. The Fastl noise was set at 66.5 dB SPL in order to obtain a signal-to-noise ratio (SNR) between the radio broadcast and the Fastl noise of -1.5. The radio broadcast consisted of conversations between several radio presenters (no music) and the amplitude varied between 64.8 and 65.6 dB SPL (playback amplitude set to 65 dB SPL); therefore, the actual SNR measured varied between -0.9 and -1.7. This was deemed as adequate for the given tasks. The additional noises (kids, baby, and mobile phone) were all played at 64 dB SPL.

The beginning of each behavioral task, the task word, and the button presses generated nonaudible trigger signals, which were sent to the data acquisition system through a trigger box (g.Trigbox, g.Tec, Austria) for *post hoc* signal processing.

E. Task Scenarios

The three main tasks were named "A," "B," and "C," each 4 min in length, involving different degrees of auditory and visual or nonauditory attentional effort while driving. Driving in task "A" was done on a highway without traffic, without speed limit, with clear weather, and without randomized traffic events. Driving in tasks "B" and "C" started on a rural road and crossed through an urban environment; for both B and C the weather was set to rain, together with fog and a sight distance limited to 40 m ahead, forcing an increased driving effort. The tasks can be summarized as follows:

1) Task "A": Driving effort—low; auditory effort—high. Driving on the highway without traffic and with a clear weather, while solving the behavioral task (pressing a button when "und" is heard) in the presence of auditory distracters.
2) Task "B": Driving effort—high; auditory effort—low. Driving on different roads with bad weather conditions;

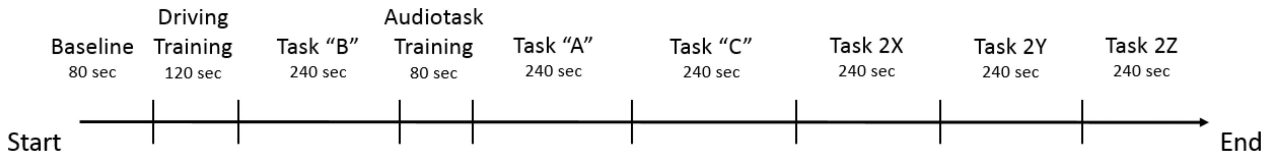

Fig. 2. Measurement plan. A baseline, two training stages, and three different tasks were performed. The three tasks (A, B, C) were repeated in a randomized order (shown here as X, Y, and Z) for retest purposes.

no auditory distracters, radio broadcast playing but button should NOT be pressed.

3) Task "C": Driving and auditory effort—high. Driving on different roads with bad weather conditions, while solving the behavioral task (pressing a button when "und" is heard) in the presence of auditory distracters.

Besides the main tasks, two training stages and an initial baseline measurement were performed.

1) Baseline: No tasks, driving simulator OFF, 80 s.
2) Driving training: Driving freely in an urban environment, 2 min.
3) Auditory training: Broadcast was presented with occurrences of the target word; participants are instructed to press the button if they detect the target word. Driving simulator OFF, 80 s.

After the main tasks were performed, tasks A, B, and C were repeated in a randomized order, as a retest to enhance the robustness of the results (referred from now on as 2A, 2B, and 2C). The scenarios and their distribution along the measurement are shown in Fig. 2.

Two subjects were measured simultaneously in each measurement (driver and copilot). Once the measurement was finished, the current driver and the copilot switched places and the measurement was restarted. Due to the subjects not being naive anymore to the measurement, the second measurement was classified differently from the first—subjects from the first measurement were classified as "round 1" (Driver and Copilot R1), and subjects from the second measurement (nonnaive) were classified as "round 2" (Driver and Copilot R2).

F. Psychophysiological Measurements

Electroencephalogram (EEG) was acquired using a high-resolution EEG system (g.HiAmp, g.Tec, Austria) with 128 active electrodes, at a sampling rate of 512 Hz. Impedances for the active electrodes were kept under 50 kΩ. No online filtering was used and all electrodes were referenced to CPz and rereferenced to the average reference postmeasurement. Additionally, two passive Ag/AgCl electrodes were placed around the left eye in order to acquire an electrooculogram (EOG), used to detect blinking.

All biosignals (EEG, EOG), together with the trigger signals from the auditory stimuli and button, and eye position tracking were acquired through the same biosignal amplifier (g.HiAmp) and controlled through a SIMULINK interface (The Mathworks, Massachusetts, MA, USA). The output file was processed using MATLAB R2013a (The Mathworks, Massachusetts, MA, USA).

G. Measurement Protocol

After the subjects read and signed the consent forms, the Ag/AgCl electrodes for EOG were placed. Afterward, the subjects were asked to sit in the driving simulator and the EEG cap was placed on their heads. The subjects received a button for solving the behavioral task; in the case of the driver, the button was fixed to the side of the index finger of the right hand. This position allowed the driver to press the button with the thumb without leaving the steering wheel.

Once all sensors were in place, the subjects were informed of the course of the measurement. They were not informed of the auditory task until the auditory training took place. Between each task, there was a small pause (approximately 1 min) where the subjects were asked if the measurement may continue. If so, the operator informed them of the upcoming task and checked that all sensors were still working correctly (e.g., impedances from the EEG and EOG electrodes remain within acceptable ranges).

At the end of the measurement, the subjects answered a small questionnaire regarding their perception of the difficulty of the tasks, their performance, the level of distraction attained through the auditory stimuli, and the quality of the simulation overall. As a safety measurement, subjects were not allowed to drive their own vehicle 30 min postmeasurement.

III. Data Processing

A. Electroencephalography

1) Signal Conditioning: The first step in the processing of the acquired (raw) EEG signals was the removal of the blinking artifacts by using independent component (IC) analysis (ICA)-based blind-source separation. This was implemented using the EEGLAB Toolbox (SCCN, San Diego, CA, USA) in MATLAB and the FastICA [51] algorithm. ICA was performed for the 128 EEG channels and the ICs were individually analyzed to search for recognizable blinking artifact patterns. Once found, these ICs were removed from the original signal. Care was taken to remove only the ICs corresponding to eye artifacts, even if in some cases the eye artifacts were not completely removed. This compromise was chosen in order to keep as much signal integrity while removing as much artifacts as possible. The output signal post-ICA was manually compared to the original EEG raw signal and to the EOG raw signal in order to confirm that the artifacts removed were indeed caused by blinking. After removing the eye artifacts, the EEG data were rereferenced to the average reference.

2) Phase–Amplitude Coupling: The PAC analysis was done following the framework established by Tort *et al.* [42]; what follows is a summary of the procedure.

In order to analyze the PAC, the EEG signal was split into three frequency bands—Theta (4–8 Hz), low Gamma (30–50 Hz), and high Gamma (50–80 Hz), using an FIR filter with a Hanning window in MATLAB. It has been argued that the useful spectrum of EEG that can be measured through scalp EEG is limited to 80 Hz [39], [43]. We split the Gamma-band analysis based on this assumption, and studied both conditions simultaneously. The mean of the filtered signals was subtracted afterward.

The Hilbert transform was applied to both Theta and Gamma acquired signals; the instantaneous phase was then extracted from the Hilbert transform of the Theta-filtered signal and the amplitude envelope was extracted from the Hilbert transform of the Gamma-filtered signal. This allows for a representation of the amplitude of the Gamma oscillations at any given phase value of the Theta oscillations.

The phase information was then split in 18 bins (each accounting for 20-degree changes) and the mean amplitude (acquired from the Gamma oscillations) over each phase bin was calculated. Finally, the mean amplitude values for each bin were normalized; the normalized amplitude acts a discrete probability density function. For no PAC, the amplitude distribution (P) over the phase bins would be uniform; therefore, a deviation from a uniform distribution denotes coupling. The deviation was calculated using the KL distance [48], adapted in order to obtain deviation values between 0 and 1. The KL distance is defined as

$$D_{KL}(P,Q) = \sum_{j=1}^{N} P(j) \log \left[\frac{P(j)}{Q(j)} \right] \tag{1}$$

where *D* is the KL distance between a discrete distribution *P* and a distribution *Q* for each element *j* in a signal of length *N*. Moreover, the KL distance can be expressed in terms of the Shannon entropy *H* of the distribution *P*, as

$$D_{KL}(P,U) = \log(N) - H(P) \tag{2}$$

where the KL distance is now expressed as the distance between the distribution *P* and the uniform distribution U. Here, $\log(N)$ corresponds to the maximal possible entropy value (uniform distribution). A modulation index (MI) is then calculated, by dividing the KL distance as expressed in (2) by $\log(N)$ as

$$MI = \frac{D_{KL}(P,U)}{\log(N)}. \tag{3}$$

For a uniform distribution of the amplitude over the phase values, the MI is zero; a value of one would correspond to a distribution centred on a specific bin (a Dirac distribution) representing a Gamma oscillation that only occurs in a single phase bin of Theta.

The MI presents very low values (as seen in [42], a "locked" Theta-phase Gamma-amplitude modulation would reach an MI value around 0.015 in ideal, simulated conditions). It is also important to note that the value is sensitive to the noise within and the length of the measurement (the measurement should have more than one cycle of the phase information). The training tasks (baseline, driving, and auditory training) are shorter (80 s) than the main tasks (240 s), and therefore, present larger MI values (longer measurements present a smaller MI variation, allowing for a stabilization of the values); the EEG information from training stages was not used for the PAC analysis due to this reason.

The MI was calculated for each channel, for each task, and for each subject, separately. Once finished, the mean for each subject group was calculated for each of the tasks (e.g., all drivers, drivers from first round separately, all copilots, and so on). The MI values were then plotted over the scalp using EEGLAB-based scripts. If an electrode had an MI value three times bigger than the average value of all electrodes, it was considered a faulty electrode; its value was then assigned based on its nearest neighbors. Measurements with more than ten faulty electrodes were not taken into account. For the final analysis, 18 of the original 22 subjects were considered, based on the quality of the measurement.

TABLE I
MEAN TASK RESULTS (IN %) FOR THE AUDITORY TASK

Group	Audio Training	A	2A	C	2C
Drivers R1	83.5	48.9	50.2	39.7	37.6
Drivers R2	82.1	56	57.3	47.6	46
D R1 + R2	82.8	52.4	53.8	43.7	41.8
Copilots R1	78.7	67.1	67.1	55.6	56.6
Copilots R2	88.3	66.7	65.8	54.5	57.7
C R1 + R2	83.5	66.9	66.4	55	57.1

IV. RESULTS

A. Behavioral Data (Detection Task)

The number of targets for each task were as follows: Training (7); Task A (25); Task C (21). Task B did not require any button presses. The task results (percentage of target words detected) are shown in Table I and represent the behavioral data of the study.

Scores for task A were higher than task C for both test and retest situations (scores for the audio training without driving were higher than both tasks A and C as expected). A repeated-measures analysis of variance (ANOVA) was performed to compare the results (in % of correct button pressings per task) between audio training, task A and C, and their retests. For each group (drivers R1, drivers R2, copilots R1, and copilots R2), the difference between tasks was significant (all $p < 0.001$ except copilot R2 $p = 0.0079$). Additionally, the difference between drivers and copilots was studied for significance as well (drivers R1 against copilots R1 and drivers R2 against copilots R2). The group difference for R1 was significant ($p = 0.0366$); the group difference for R2 did not reach significance ($p = 0.2176$).

The questionnaires filled out by the participants after the measurement contained questions rated on a five-point scale. The participants described on average the difficulty to solve the behavioral task as very easy during task A (highway) and easy/mild during task C (mixed road with bad weather). Of the

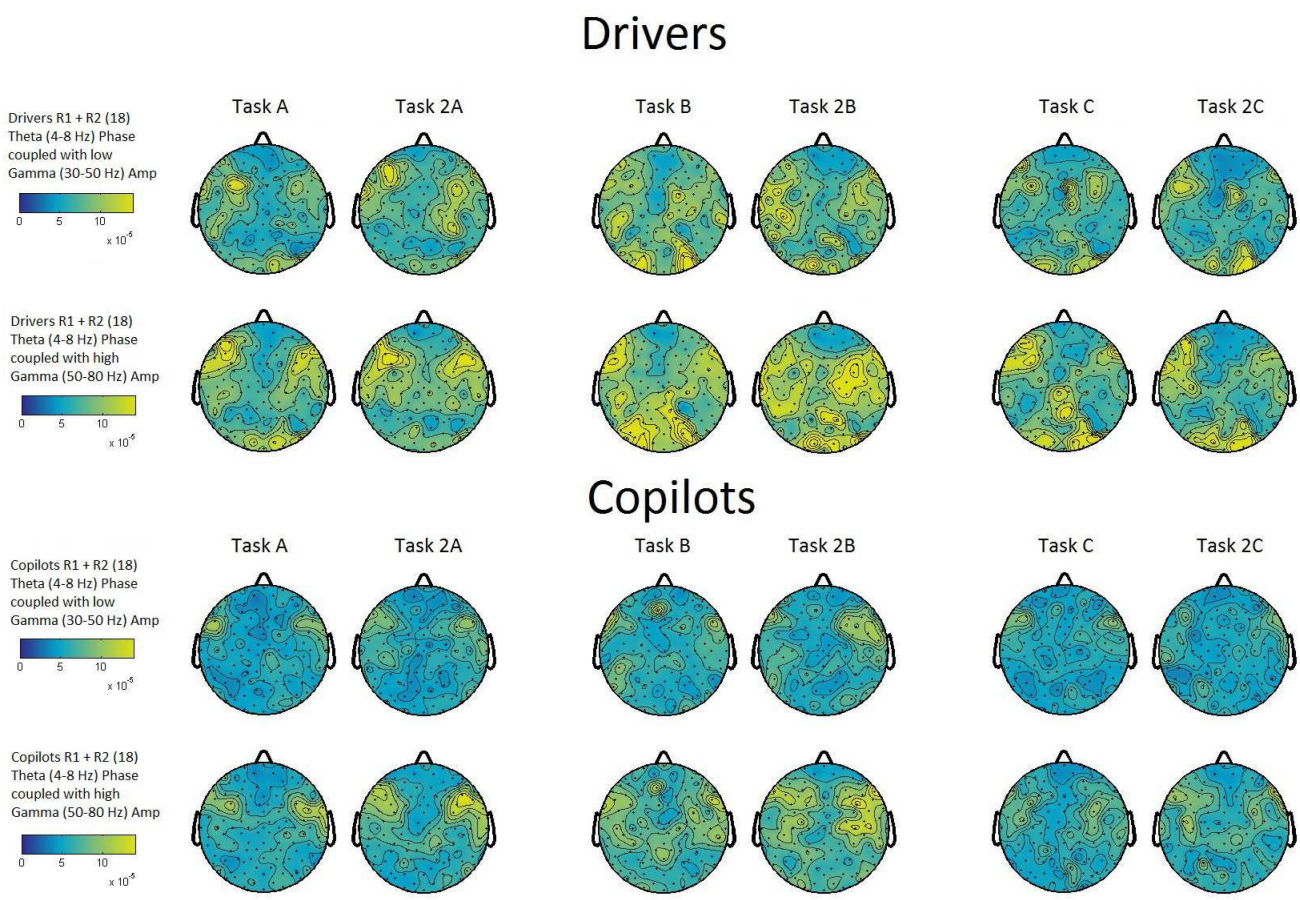

Fig. 3. PAC results for all driver and copilots, main tasks. MI is truncated to 0.00014 for clarity. Low (above) and high (below) Gamma amplitudes are shown, for all tasks.

22 subjects, 19 rated the weather as having a low influence on their driving performance (1/5) while three subjects rated it as having a strong influence (5/5). Compared to the behavioral task results, subjects overestimated their performance and level of distraction.

B. Phase–Amplitude Coupling

Fig. 3 shows the PAC results for all drivers (R1 and R2 combined), and all copilots (R1 and R2 combined), for all tasks. Fig. 4 shows the results for drivers only, comparing R1 and R2 rounds.

C. PAC Statistical Analysis

To assess if there was indeed a significant difference between drivers and copilots in general, a mixed ANOVA test using the PAC value of each single electrode as the dependent variable was used (between-subjects factor—driver/copilot; within-subjects-factor—tasks). The difference between drivers "R1" and "R2" was again assessed using a mixed-ANOVA test (between-subjects factor—drivers R1/R2; within-subjects factor—tasks). In order to assess significant differences between single tasks, one-way repeated measures ANOVA was used between all tasks (again using the PAC value of each electrode as the dependent variable); drivers and copilots were analyzed separately.

Nine regions of interest (ROIs) were defined to present the results—dorsolateral prefrontal cortex left (DLPFC L) and right (DLPFC R), frontal eye fields left (FEF L) and right (FEF R), superior frontal gyrus (SFG), primary motor cortex left (PMC L) and right (PMC R), and primary visual cortex left (PVC L) and right (PVC R). Electrodes that presented significant differences in the statistical analysis were grouped into each ROI and accounted for. The ROIs are shown in Fig. 5 and the number of electrodes with significant differences are shown in Fig. 6.

Given the results from the repeated measures ANOVA test, significant differences between the first and second round of each task were additionally investigated using a paired-T test (comparison between test and retest). Results are shown in Figs. 7 (drivers) and 8 (copilots).

V. Discussion

The behavioral data (results on the detection task) showed a significant difference between the pure auditory task (training, without driving) and the multimodal tasks (A and C), which allows to confirm that the tasks were distinct enough and that task

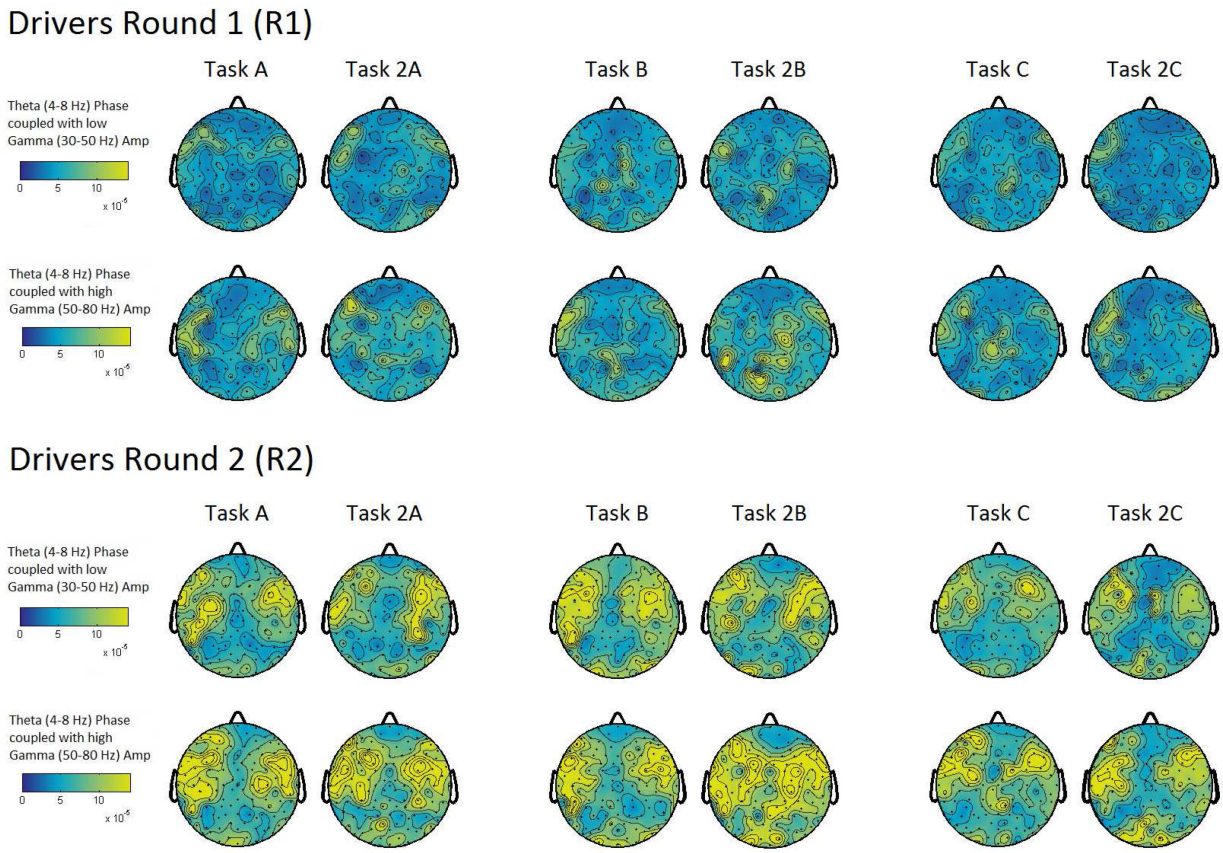

Fig. 4. PAC results for drivers from rounds 1 and 2 separately. Modulation index is truncated to 0.00014 for clarity. Low (above) and high (below) Gamma amplitudes are shown, for all tasks.

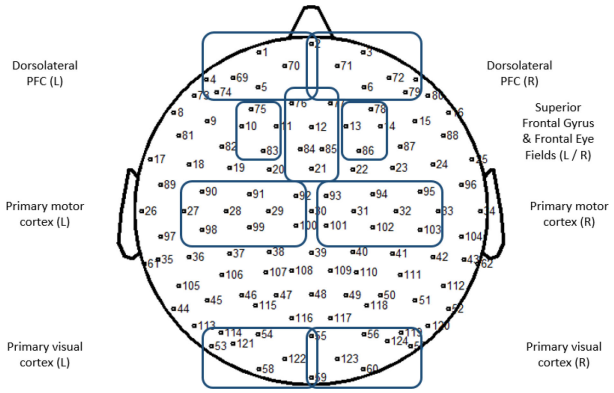

Fig. 5. Regions of interest defined for the statistical analysis.

C was more difficult than A (as seen in the scores). It also showed a high retest reliability in both tasks A and C (see Table I). A significant difference was also found between drivers and copilots for the first round.

Regarding PAC indices and focusing on the Theta/high Gamma band, an overall higher activation was seen in drivers (both R1 and R2) compared to copilots, especially in occipital areas; activation on prefrontal and parietal areas was observed on both, but reduced in copilots (see Fig. 3). Electrodes showing significant PAC differences were found in prefrontal, primary motor cortex, frontal eye fields, and occipital areas, confirming the main hypothesis of this article, which suggested that PAC might be a suitable biomarker for attention-related cortical activation. From the Gamma subdivisions chosen, the high-Gamma domain (50–80 Hz) offered the most recognizable differences overall, as seen by the number of electrodes with significant differences (see Fig. 6). For example, the PMC R region presented six electrodes out of ten with significantly higher PAC when observed in the high-Gamma domain, compared to one single electrode out of ten in the low-Gamma band for the same region. Significant differences between drivers and copilots were found in the same regions both for low and high Gamma (motor area, left prefrontal cortex, and occipital area); however, as previously discussed and as seen in Fig. 6, a higher number of electrodes within the high-Gamma band presented a significant PAC difference.

The observation regarding the high-Gamma band agrees with the literature regarding cross-frequency coupling, where usually electrocorticography (ECOG) is preferred and higher Gamma-band components are taken into account; it has been discussed that surface EEG cannot provide reliable signal components above 80 Hz [39], [43]. Our results suggest that the Gamma range between 50 and 80 Hz might provide enough information for cross-frequency coupling, even when using surface EEG.

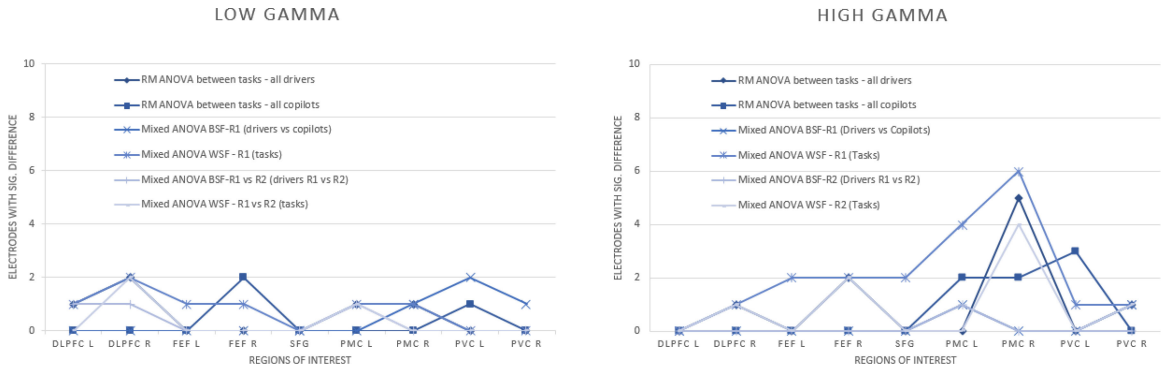

Fig. 6. Number of electrodes presenting significant differences in PAC, for each ROI. The ROIs are DLPFC L, DLPFC R, FEF L, FEF R, SFG, PMC L, PMC R, PVC L, and PVC R. (Right) A higher number of electrodes presented significant differences in PAC within the high-Gamma band (6) compared to the same region when limited to the low-Gamma band (1), thus, suggesting that a stronger PAC is seen in the high-Gamma (50–80 Hz) range.

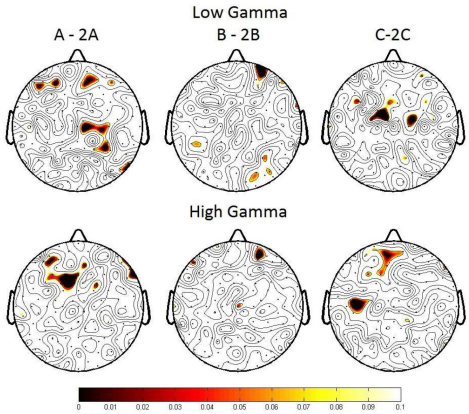

Fig. 7. (Drivers) Paired-T test results between test and retest of each task, for low (above) and high (below) Gamma.

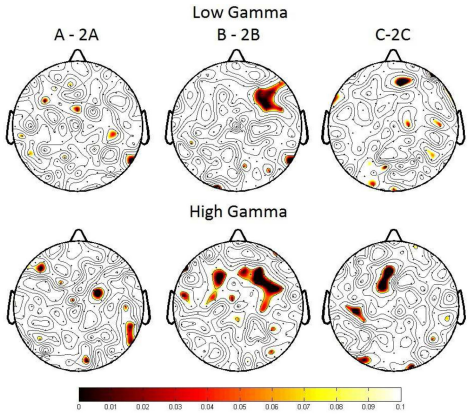

Fig. 8. (Copilots) Paired-T test results between test and retest of each task, for low (above) and high (below) Gamma.

When analyzing drivers R1 against drivers R2, R2 showed overall higher PAC (see Fig. 4) in prefrontal and parietal areas. Since these participants knew the tasks beforehand, this finding might perhaps indicate an increased motivation/effort to solve the tasks correctly. This agrees with the behavioral data; the scores were reduced for the multimodal tasks suggesting an increased effort to solve the task. However, there was no significant difference in the PAC in the occipital areas when comparing R1 and R2 drivers (mixed ANOVA, between subject factor), which may indicate that a similar effort is required for the driving task as compared to R1, and reduced (but present) significant differences in the prefrontal cortex and left parietal cortex. The PAC difference between tasks between R1 and R2 was significant on the right prefrontal cortex, right frontal eye fields, right primary motor cortex, and right primary visual cortex as well (mixed ANOVA, within subject factor).

Significant differences between the test and retest of each task (see Figs. 7 and 8) were found, albeit strictly localized. For drivers, significant differences were found mostly in the prefrontal cortex and motor area. For copilots, significant differences were found in the frontal eye field region for task B and C in the high-Gamma band. This might suggest a learning effect in the retest stages. Moreover, this might explain why the difference in behavioral data between drivers and copilots was not significant for the second round. Prefrontal areas presented activity during most of the tasks, both for drivers and copilots. This agrees with the idea of assessing working memory-involved tasks through PAC, which include executive, integrative, and storage functions simultaneously [19], [45]. Left dorsolateral prefrontal cortex showed a significant difference between all tasks for the drivers only; this might point to different resource allocations during a multimodal task (trying to drive in taxing weather conditions while solving an auditory task).

Opposed to our secondary hypothesis, we did not find an increased PAC around the auditory cortex areas in the low-driving effort/high-auditory effort tasks. A reason might be either a prioritization of visual attention or the lack of a “pure” auditory stimulation, instead being replaced by multimodal stimulation. The main objective of the auditory task was to provide a distraction to the driving task and to act as a behavioral task to rate the difficulty of scenarios. There might also not have been enough contrast between the auditory task and the distraction, rendering the task easy to solve. However, this contradicts the behavioral task results, which show a lower success rate for tasks A and C compared to pure auditory tasks (see Table I). The designed

auditory task corresponds more strictly to a detection task, which might not elicit the same effort compared to an auditory scene analysis task [52].

Additional drawbacks of the current study are given by the spatial distribution of the sensors. Whereas a 128-electrode system offers good spatial resolution, the measured PAC can be influenced by volume conduction and correct placement of electrodes for each measurement and their performance during the complete length of the study. Both factors increase the variability of the results. The obtained results provide an insight of areas showing increased PAC, but they would greatly benefit from comparison to studies using more in-depth (e.g., invasive or combined with MEG) measurements. Moreover, as explained by Tort *et al.* in [42] and as seen in the PAC results for the baseline and training stages, the PAC scale is sensitive to time resolution, i.e., shorter measurements present higher PAC indices due to less cycles available for each frequency band and an increased SNR (although the ratio of activation between coupled and noncoupled areas seems to be conserved). This is due to the MI's dependence on the length of the signal (in this case, the length of the EEG measurement). Tort *et al.* suggest either a minimum of 30 s, or more than 200 cycles for Theta-band analysis. While our baseline and training stages (80 and 120 s) fulfill the criteria, longer measurements (such as the main tasks with 240 s) provided more accurate results.

VI. Conclusion

A higher PAC index was observed in the EEG from drivers, for prefrontal (DLPFC, FEF), parietal (PMC), and occipital (PVC) areas, especially on tasks B and 2B (pure driving tasks). The high-Gamma range (50–80 Hz) seems to be more sensitive to phase locking analysis than low Gamma as judged by the number of electrodes with significantly different PAC indices. Copilots presented an overall lower cortical activation, specifically in the occipital area compared to the pilots; this might indicate a reduced cognitive load for visual tasks and a focus on the context of the behavioral task (prefrontal activity).

The hypothesis of PAC as a biomarker of attention-related cortical activation was confirmed by the region-locked results, especially within the high-Gamma band. Additional significance measures were able to selectively detect areas of interest such as the frontal eye fields, the primary motor cortex, and the primary visual cortex. The study allowed the identification of areas in which PAC can be measured and might be easily implemented in real driving situations; this information might be used in driver-assistance systems to enhance safety. The nonnaive drivers (Round 2) presented an overall higher PAC, which might also suggest PAC as a tool to isolate different multimodal cognitive effort; however, the expected activity in the auditory cortex was not found.

Future work should be focused on increasing the reliability of PAC as a biomarker for attention in multimodal tasks. Coupling between different brain areas, which has been shown to have effect in processes such as memory encoding [53] should also be studied. Future work might also include the analysis of PAC in nondriving modality-specific tasks (e.g., pure auditory stimulation) and their comparison to multimodal tasks.

References

[1] T. A. Schweizer, K. Kan, Y. Hung, F. Tam, G. Naglie, and S. J. Graham, "Brain activity during driving with distraction: An immersive fMRI study," *Frontiers Human Neurosci.*, vol. 7, no. 53, pp. 1–11, 2013.

[2] L. Tijerina, S. Johnston, E. Parmer, and M. D. Winterbottom, "Driver distraction with wireless telecommunications and route guidance systems," Nat. Highway Traffic Saf. Admin., U. S. Dept. Transp., Washington, DC, USA, Tech. Rep. DOT HS 809-0692, 2000.

[3] W. J. Horrey and C. D. Wickens, "Driving and side task performance: The effects of display clutter, separation, and modality," *Human Factors*, vol. 46, no. 4, pp. 611–624, 2004.

[4] J. M. Owens, S. B. McLaughlin, and J. Sudweeks, "Driver performance while text messaging using handheld and in-vehicle systems," *Accident Anal. Prevention*, vol. 43, pp. 939–947, 2011.

[5] D. V. McGehee, "Visual and cognitive distraction metrics in the age of the smart phone: A basic review," *Ann. Adv. Automot. Med.*, vol. 58, pp. 15–23, 2014.

[6] K. Young and M. Regan, "Driver distraction: A review of the literature," in *Distracted Driving*, I. J. Faulks, M. Regan, M. Stevenson, J. Brown, A. Porter, and J. Irwin, Eds. Sydney, NSW, Australia: Australas. College Road Saf., 2007, pp. 379–405.

[7] P. Sagaspe *et al.*, "Extended driving impairs nocturnal driving performances," *PLoS One*, vol. 3, no. 10, pp. 1–6, 2008.

[8] C. T. Lin *et al.*, "Mind wandering tends to occur under low perceptual demands during driving," *Sci. Rep.*, vol. 17, no. 6, 2016, Art. no. 21353.

[9] V. D. Calhoun, V. B. McGinty, and G. D. Pearlson, "Driving and the brain: An imaging study," in *Proceedings of the 1st Human-Centered Transportation Simulation Conference, The University of Iowa, Iowa City, Iowa, November 4–7, 2011*.

[10] V. D. Calhoun and G. D. Pearlson, "A selective review of simulated driving studies: Combining naturalistic and hybrid paradigms, analysis approaches, and future directions," *NeuroImage*, vol. 59, pp. 25–35, 2012.

[11] M. A. Just, T. A. Keller, and J. Cynkar, "A decrease in brain activation associated with driving when listening to someone speak," *Brain Res.*, vol. 1205, pp. 70–80, 2008.

[12] S. C. Chung *et al.*, "Effects of distraction task on driving: A functional magnetic resonance imaging study," *Bio-Med. Mater. Eng.*, vol. 24, pp. 2971–2977, 2014.

[13] S. M. Bowyer *et al.*, "Conversation effects on neural mechanisms underlying reaction time to visual events while viewing a driving scene using MEG," *Brain Res.*, vol. 1251, pp. 151–161, 2009.

[14] A. Fort *et al.*, "Attentional demand and processing of relevant visual information during simulated driving: A MEG study," *Brain Res.*, no. 1363, pp. 117–127, 2010.

[15] K. Sakihara *et al.*, "Cerebral oscillatory activity during simulated driving using MEG," *Frontiers Human Neurosci.*, vol. 8, no. 975, pp. 1–9, 2014.

[16] B. T. Jap, S. Lal, P. Fischer, and E. Bekiaris, "Using EEG spectral components to assess algorithms for detecting fatigue," *Expert Syst. Appl.*, vol. 36, pp. 2352–2359, 2009.

[17] C. T. Lin, S. A. Chen, T. T. Chiu, H. Z. Lin, and L. W. Ko, "Spatial and temporal EEG dynamics of dual-task driving performance," *J. NeuroEng. Rehabil.*, vol. 8, no. 11, pp. 1–13, 2011.

[18] C. T. Lin, R. C. Wu, T. P. Jung, S. F. Liang, and T. Y. Huang, "Estimating driving performance based on EEG spectrum analysis," *EURASIP J. Appl. Signal Process.*, vol. 19, pp. 3165–3174, 2005.

[19] S. Lei and M. Roetting, "Influence of task combination on EEG spectrum modulation for driver workload estimation," *Human Factors*, vol. 53, no. 2, pp. 168–179, 2011.

[20] G. Li and W. Y. Chung, "A context-aware EEG headset system for early detection of driver drowsiness," *Sensors*, vol. 15, pp. 20873–20893, 2015.

[21] E. Wascher, S. Getzmann, and M. Karthaus, "Driver state examination—Treading new paths," *Accident Anal. Prevention*, vol. 91, pp. 157–165, 2016.

[22] J. M. Morales *et al.*, "Monitoring driver fatigue using a single-channel electroencephalographic device: A validation study by gaze-based, driving performance, and subjective data," *Accident Anal. Prevention*, vol. 109, pp. 62–69, 2017.

[23] K. Yoshino, N. Oka, K. Yamamoto, H. Takahashi, and T. Kato, "Functional brain imaging using near-infrared spectroscopy during actual driving on an expressway," *Frontiers Human Neurosci.*, vol. 7, no. 882, pp. 1–16, 2013.

[24] N. Oka *et al.*, "Greater activity in the frontal cortex on left curves: A vector-based fNIRS study of left and right curve driving," *PLoS One*, vol. 10, no. 5, 2015, Art. no. e0127594.
[25] R. Nosrati, K. Vesely, T. Schweizer, and V. Toronov, "Event-related changes of the prefrontal cortex oxygen delivery and metabolism during driving measured by hyperspectral fNIRS," *Biomed. Opt. Exp.*, vol. 7, no. 4, pp. 1323–1335, 2016.
[26] S. Ahn, T. Nguyen, H. Jang, J. G. Kim, and S. C. Jun, "Exploring neuro-physiological correlates of drivers' mental fatigue caused by sleep deprivation using simultaneous EEG, ECG and fNIRS data," *Frontiers Human Neurosci.*, vol. 10, no. 219, pp. 1–14, 2016.
[27] A. K. Engel, P. Fries, and W. Singer, "Dynamic predictions: Oscillations and synchrony in top–down processing," *Nature Rev. Neurosci.*, vol. 2, pp. 704–718, 2001.
[28] C. Tallon-Baudry, O. Bertrand, C. Delpuech, and J. Pernier, "Oscillatory gamma-band (30–70 Hz) activity induced by a visual search task in humans," *J. Neurosci.*, vol. 17, no. 2, pp. 722–734, 1997.
[29] T. Gruber, M. M. Müller, A. Keil, and T. Elbert, "Selective visual-spatial attention alters induced gamma band responses in the human EEG," *Clin. Neurophysiol.*, vol. 110, pp. 2074–2085, 1999.
[30] C. S. Herrmann, M. H. K. Munk, and A. K. Engel, "Cognitive functions of gamma-band activity: Memory match and utilization," *Trends Cogn. Sci.*, vol. 8, no. 8, pp. 347–355, 2004.
[31] O. Jensen, J. Kaiser, and J. P. Lachaux, "Human gamma-frequency oscillations associated with attention and memory," *Trends Neurosci.*, vol. 30, no. 7, pp. 317–324, 2007.
[32] W. Klimesch, "EEG alpha and theta oscillations reflect cognitive and memory performance: A review and analysis," *Brain Res. Rev.*, vol. 29, pp. 169–195, 1999.
[33] M. X. Cohen, "Error-related medial frontal theta activity predicts cingulate-related structural connectivity," *NeuroImage*, vol. 55, pp. 1373–1383, 2011.
[34] M. Gärtner, L. Rohde-Liebenau, S. Grimm, and M. Bajbouj, "Working memory-related frontal theta activity is decreased under acute stress," *Psychoneuroendocrinology*, vol. 43, pp. 105–113, 2014.
[35] P. Arrighi *et al.*, "EEG theta dynamics within frontal and parietal cortices for error processing during reaching movements in a prism adaptation study altering visuo-motor predictive planning," *PLoS One*, vol. 11, no. 3, pp. 1–27, 2016.
[36] G. Buzsáki and A. Draguhn, "Neuronal oscillations in cortical networks," *Science*, vol. 304, no. 5679, pp. 1926–1929, 2013.
[37] P. Fries, "A mechanism for cognitive dynamics: Neuronal communication through neuronal coherence," *Trends Cogn. Sci.*, vol. 9, no. 10, pp. 474–480, 2005.
[38] P. J. Uhlhaas, F. Roux, E. Rodriguez, A. Rotarska-Jagiela, and W. Singer, "Neural synchrony and the development of cortical networks," *Trends Cogn. Sci.*, vol. 14, no. 2, pp. 72–80, 2009.
[39] O. Jensen and L. L. Colgin, "Cross-frequency coupling between neuronal oscillations," *Trends Cogn. Sci.*, vol. 11, no. 7, pp. 267–269, 2007.
[40] M. X. Cohen, "Assessing transient cross-frequency coupling in EEG data," *J. Neurosci. Methods*, vol. 168, pp. 494–499, 2008.
[41] V. Jirsa and V. Müller, "Cross-frequency coupling in real and virtual brain networks," *Frontiers Comput. Neurosci.*, vol. 7, no. 78, pp. 1–25, 2013.
[42] A. B. L. Tort, R. Komorowski, H. Eichenbaum, and N. Kopell, "Measuring phase-amplitude coupling between neuronal oscillations of different frequencies," *J. Neurophysiol.*, vol. 104, pp. 1195–1210, 2010.
[43] R. T. Canolty *et al.*, "High gamma power is phase-locked to theta oscillations in human neurocortex," *Science*, vol. 313, pp. 1626–1628, 2006.
[44] J. Lisman, "The theta/gamma discrete phase code occuring during the hippocampal phase precession may be a more general brain coding scheme," *Hippocampus*, vol. 15, pp. 913–922, 2005.
[45] S. I. Dimitriadis, Y. Sun, K. Kwok, N. Laskaris, N. Thakor, and A. Bezerianos, "Cognitive workload assessment based on the tensorial treatment of EEG estimates of cross-frequency phase interactions," *Ann. Biomed. Eng.*, vol. 43, no. 4, pp. 977–989, 2015.
[46] A. Bruns and R. Eckhorn, "Task-related coupling from high- to low-frequency signals among visual cortical areas in human subdural recordings," *Int. J. Psychophysiol.*, vol. 51, pp. 97–116, 2004.
[47] T. Demiralp *et al.*, "Gamma amplitudes are coupled to theta phase in human EEG during visual perception," *Int. J. Psychophysiol.*, vol. 64, pp. 24–30, 2007.
[48] S. Kullback and R. A. Leibler, "On information and sufficiency," *Ann. Math. Statist.*, vol. 22, pp. 79–86, 1951.
[49] A. Ruoff, *Häufigkeitswörterbuch Gesprochener Sprache: Gesondert Nach WOrtarten, Alphabetisch, Rückläufig Alphabetisch und Nach Häufigkeit Geordnet*. Berlin, Germany: de Gruyter (in German), 1981.
[50] H. Fastl, "A background noise for speech audiometry," *Audiol. Acoust.*, vol. 26, pp. 2–13, 1987.
[51] A. Hyvärinen and E. Oja, "Independent component analysis: Algorithms and applications," *Neural Netw.*, vol. 13, pp. 411–430, 2000.
[52] C. Bernarding, D. J. Strauss, R. Hannemann, H. Seidler, and F. I. Corona-Strauss, "Neurodynamic evaluation of hearing aid features using EEG correlates of listening effort," *Cogn. Neurodyn.*, vol. 11, no. 3, pp. 203–215, 2017.
[53] U. Friese, M. Köster, U. Hassler, U. Martens, N. Trujillo-Barreto, and T. Gruber, "Successful memory encoding is associated with increased cross-frequency coupling between frontal theta and posterior gamma oscillations in human scalp-recorded EEG," *Neuroimage*, vol. 66, pp. 642–647, 2013.